

## Control of Etch Slope during Etching of Pt in Ar/Cl<sub>2</sub>/O<sub>2</sub> Plasmas

Won Jong YOO, Jin Hwan HAHM, Hyoun Woo KIM, Chan Ouk JUNG,  
Young Bum KOH and Moon Yong LEE

Semiconductor Research and Development Center, Samsung Electronics Co. Ltd.,  
San #24, Nongseo-Ri, Kiheung-Eup, Yongin-Goon, Kyungki-Do 449-900, Korea

(Received October 31, 1995; accepted for publication February 15, 1996)

Pt patterns of the 0.25  $\mu\text{m}$  design rule were etched at 20°C using a magnetically enhanced reactive ion etcher. The main problem of this device integration process is the redeposition of the etch products onto the pattern sidewall, making it difficult to reduce the pattern size. In both cases using a photoresist mask and an oxide mask, the redeposits of the etch products onto the sidewall were reduced by the addition of Cl<sub>2</sub> to Ar, although the etch slope was lowered to 45°. Using the oxide mask, by adding O<sub>2</sub> to the Cl-containing gas, the etch slope was increased up to 70°, and the redeposits were removed by an HCl cleaning process.

KEYWORDS: Pt, etching, semiconductor, sputtering, redeposition, model, sidewall, slope, chlorine, oxygen

### 1. Introduction

Small-feature-size dynamic random access memory (DRAM) devices require capacitors of larger capacitance, and this has resulted in more complicated device structures such as cylinders or trenches which involve many difficult process steps. To avoid stringent process requirements associated with conventional capacitor structures that utilize low dielectric materials such as oxide/nitride, high dielectric capacitors with stack structures are being developed.<sup>1)</sup>

Barium strontium titanate (BSTO or BST<sup>1-4</sup>) hereafter) is an appropriate material for stack capacitors because its dielectric constant is higher than 400. Platinum is used as an electrode material because it is inert to oxidation which tends to occur due to high diffusivity of BST in subsequent high temperature processes. Also, Pt is known to have leakage current lower than those of other electrodes such as RuO<sub>2</sub><sup>5,6)</sup> and poly-Si. However, non-reactivity of Pt has proved to be disadvantageous for plasma etching since no volatile etch products can be easily formed.

According to recent studies,<sup>2,7,8)</sup> the etching of Pt appears to be possible only by the sputter process, which usually results in unwanted sidewall redeposits. These sidewall redeposits were found to have thicknesses of 100 to 300 Å, and could be deleterious since they limit the definition of subquarter micron etch patterns. In addition, the sharp profiles formed by the redeposits prevented the subsequent deposition of BST films thinner than 400 Å. The appropriate etch slopes for device integration appeared to range from 65° to 80° after the removal of the sidewall redeposits. This study shows that the sidewall redeposition during Pt etching is reduced in Cl-rich plasmas at low pressure, and that the etch slope of Pt is increased by the addition of O<sub>2</sub> to Cl<sub>2</sub>/Ar. It was possible to integrate the patterned Pt into the Pt/BST capacitor structure of 0.25  $\mu\text{m}$  DRAM devices.

### 2. Experiment

A magnetically enhanced reactive ion etcher (MERIE) was used for the etching of Pt. The chiller temperature was fixed at 20°C. Figure 1 illustrates the test structure with Pt as the storage node and cell plate, and BST as

the dielectric. The Pt films were deposited by RF sputtering and patterned by either photoresist or oxide mask depending on the etchant gas. With Ar/CF<sub>4</sub> and Ar/Cl<sub>2</sub>, the oxide mask was used for improving the etch slope by minimizing the oxide consumption, otherwise the photoresist mask was used. However, with Ar/Cl<sub>2</sub>/O<sub>2</sub> the oxide mask was always used. The thicknesses of Pt and BST were in the range of 500 Å to 1000 Å. Ti film of 100 Å was deposited by sputtering to ensure the adhesion of Pt to SiO<sub>2</sub>, and TiN of 100 Å was also deposited by sputtering as a barrier to interdiffusion between Pt and the poly-Si plug (Fig. 1). Etching of Pt was carried out in the pressure range of 5 to 40 mTorr, magnetic strength of 80 Gauss, and total gas flow of 50 sccm. For the etching of Pt, etchant gases such as Ar, CF<sub>4</sub>, Cl<sub>2</sub>, and O<sub>2</sub> were introduced into the MERIE chamber. RF power was in the range of 300 to 1000 W. The RF power was switched off after 30% overetching to completely remove Pt as well as the underlying Ti/TiN films. The endpoint was determined by an optical emission detector directed parallel to the center of the wafer and 5 mm above it. After the etching of Pt, the oxide mask was removed by diluted HF, and the redeposits remaining on the sidewall, if any, were removed by 20% HCl.

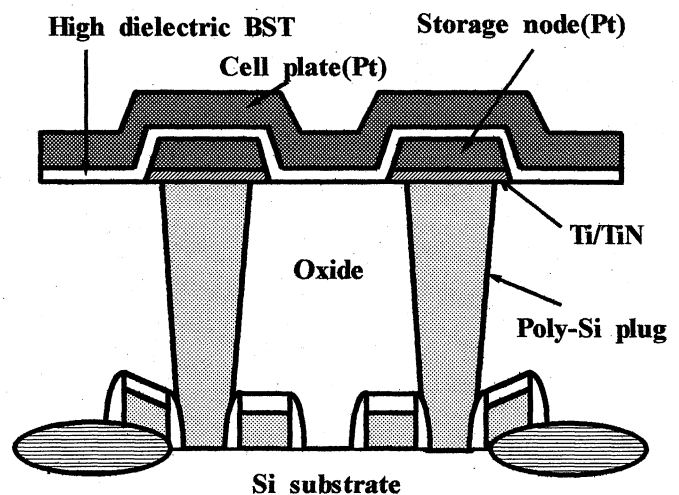


Fig. 1. Pt/BST capacitor structure.

### 3. Results

#### 3.1 Addition of halogenated gases to Ar

Inert materials such as Au and Pt were known to be etched predominantly by the sputter process, and thus far, their etch mechanisms have been studied extensively in Ar plasmas.<sup>9,10</sup> Figure 2(a) shows an etch profile obtained with the Ar plasma using the photoresist mask. The sidewall redeposits of 200 Å thickness remained even after ashing the photoresist off. With the addition of CF<sub>4</sub> to Ar, the sidewall redeposition also occurred for both photoresist and oxide masks, and the redeposits could not be removed by subsequent wet cleaning. Halogenated gas (either CF<sub>4</sub> or Cl<sub>2</sub>) of concentration ranging up to 100% was added to Ar at a pressure of 10 mTorr and an RF power of 500 W.

Figure 3 shows Auger electron spectroscopy (AES) spectra revealing the chemical components of the sidewall redeposits which are left after removing the oxide mask by diluted HF. Most of the chemical components

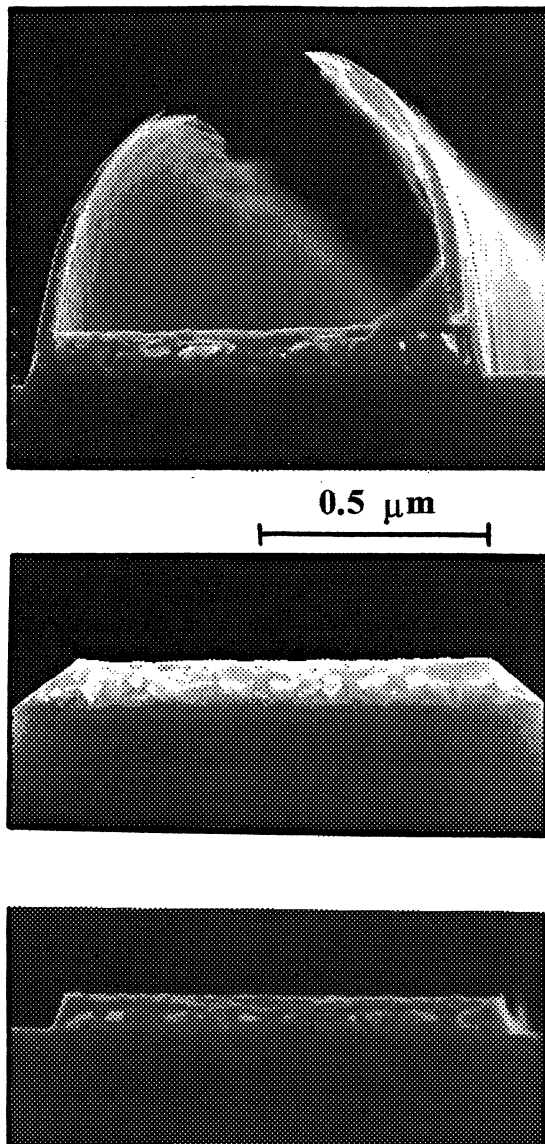


Fig. 2. SEM micrographs of Pt patterns after etching and ashing in (a) 100% Ar (b) 40% Ar + 60% Cl<sub>2</sub> (c) 80% O<sub>2</sub> + 20% Cl<sub>2</sub>.

were Pt with some traces of O which may have originated from the oxide mask. F was not detected although 40% of CF<sub>4</sub> was added to Ar, implying that no etch products in the form of PtF<sub>x</sub> were formed during the etch process. For AES, the sample was tilted up to 60° to expose sidewall redeposits thicker than 200 Å on the Pt lines thicker than 5 microns. The Auger electron beam was less than 2 microns in diameter, and was confined only on the sidewall redeposits. Figure 3 also shows the AES result after an *in situ* sputtering of 200 Å of the redeposits. This was to ensure the precise analysis of the sample which was contaminated during handling.

On the other hand, with Cl<sub>2</sub>/Ar the sidewall redeposits were removed although the etch slope was lowered to only about 45°. The etch rates of Pt were decreased by the addition of either CF<sub>4</sub> or Cl<sub>2</sub>. The etch rates were 1150 Å/min for Ar, 150 Å/min for CF<sub>4</sub>, and 500 Å/min for Cl<sub>2</sub>. The addition of Cl<sub>2</sub> resulted in less sidewall redeposits which could be removed with the ashing process of the photoresist mask followed by a conventional wet cleaning process, as shown in Fig. 2(b).

#### 3.2 Etch slope with addition of O<sub>2</sub> to Ar/Cl<sub>2</sub>

Although the use of Cl<sub>2</sub> enabled the removal of the sidewall redeposits, the etch slope was reduced by the addition of Cl<sub>2</sub> to Ar (Fig. 2(b)). For example, the etch slope was about 45° for 60% Cl<sub>2</sub> in Ar.

In order to increase the etch slope, O<sub>2</sub> was added to Ar/Cl<sub>2</sub>, while the concentration of Cl<sub>2</sub> remained constant at 20%. The concentrations of Ar and Cl<sub>2</sub> ranged from 0% to 80% at a pressure of 10 mTorr, an RF power of 500 W, and a magnetic field of 80 Gauss. Figure 4 shows that the etch rates of both Pt and SiO<sub>2</sub> decreased as the concentration of O<sub>2</sub> increased, but the etch rate of SiO<sub>2</sub> decreased faster than that of Pt. For example, the etch rate of Pt decreased from 1200 Å/min for 0% O<sub>2</sub> to 350 Å/min for 80%, whereas the etch rate of the mask oxide decreased from 1500 Å/min to 300 Å/min. Also, Fig. 5 illustrates the change in the etch slope obtained with the oxide mask when O<sub>2</sub> was added to Ar/Cl<sub>2</sub>. The addition of O<sub>2</sub> brought about increases in the etch slope of the Pt patterns and in the etch selectivity of Pt with respect to the oxide mask. The etch slope increased from 45° for 0% O<sub>2</sub> to 80° for 80% O<sub>2</sub>, while the etch selectivity increased from 0.77 to 1.17. The SEM micrograph of

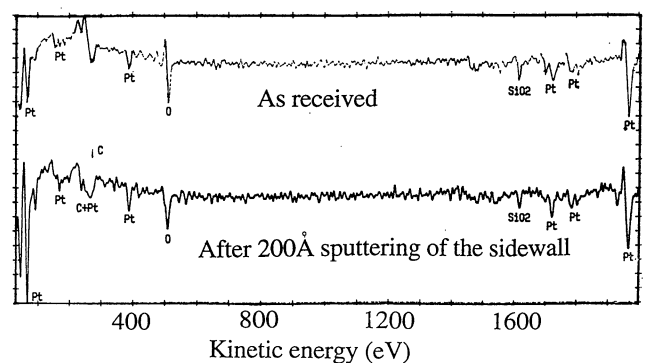


Fig. 3. AES spectra of the sidewall redeposits after etching of Pt (CF<sub>4</sub> 40%, Ar 60%).

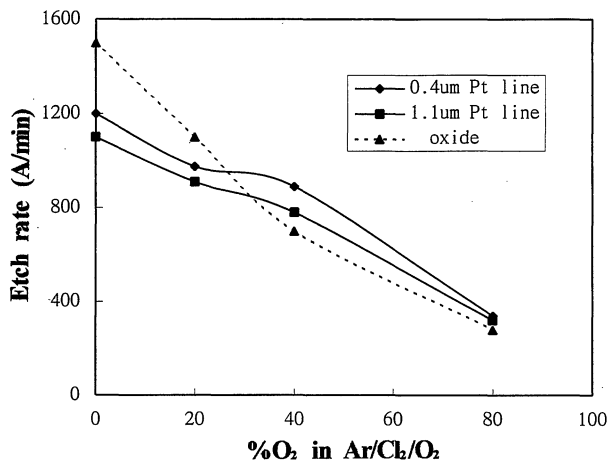


Fig. 4. Etch rates of the 0.4 μm Pt line, the 1.1 μm Pt line, and the SiO<sub>2</sub> mask as a function of % O<sub>2</sub> in Ar + Cl<sub>2</sub> + O<sub>2</sub>.

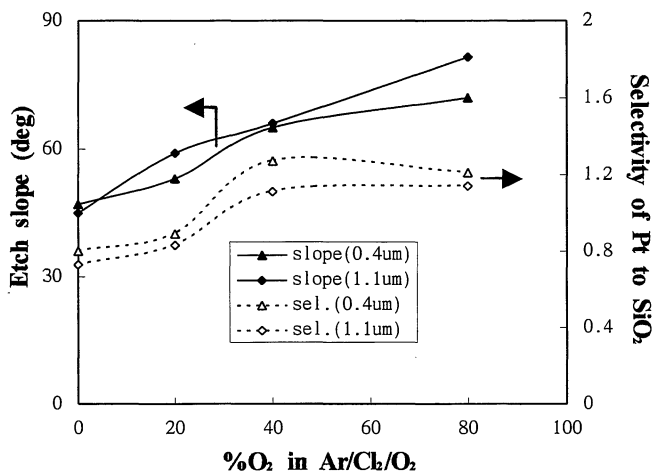


Fig. 5. Etch slopes of 0.4 μm and 1.1 μm Pt lines and etch selectivities with respect to SiO<sub>2</sub> mask as a function of % O<sub>2</sub> in Ar + Cl<sub>2</sub> + O<sub>2</sub>.

Fig. 2(c) shows the increase of the etch slope due to the addition of O<sub>2</sub>. It appears that, when the etching of Pt and SiO<sub>2</sub> proceeds predominantly via the sputter process, some of the etch products of the SiO<sub>2</sub> mask can be mixed into the sidewall redeposits, as evidenced by the AES results in Fig. 3. An increase in the selectivity with less consumption of SiO<sub>2</sub> mask brings about the thinner sidewall redeposits, resulting in steeper etch profiles.

In Fig. 5 the etch slope in 0.4 μm lines was lower by about 3° to 5° than that in 1.1 μm lines. For Pt patterns used as storage nodes in the devices, the etch slopes were 61° for 0.25 μm, 67° for 0.3 μm, and 71° for 0.4 μm patterns. Dependence of the etch slope on the pattern size is under investigation.

### 3.3 Process integration

It was essential to detect the endpoint of the etching of Pt to minimize the consumption of the underlying oxide dielectric, as shown in Fig. 1. We found that, at 10 mTorr the optical emission intensity at 3406 Å was sharply decreased when Pt was completely etched. Figure 6 shows the time evolution of the optical emission intensity dur-

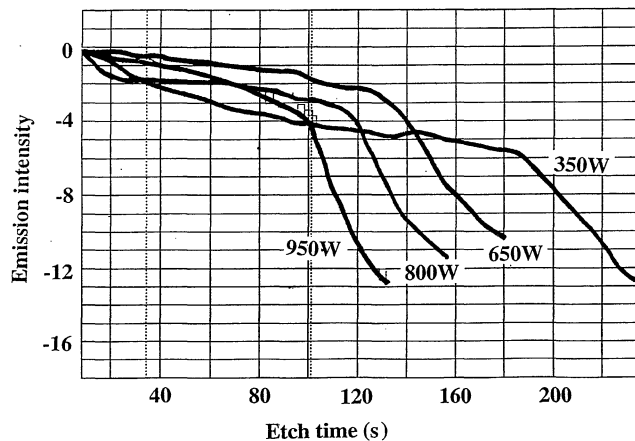


Fig. 6. Time evolution of 3406 Å optical emission intensity during etching of Pt at various RF powers.

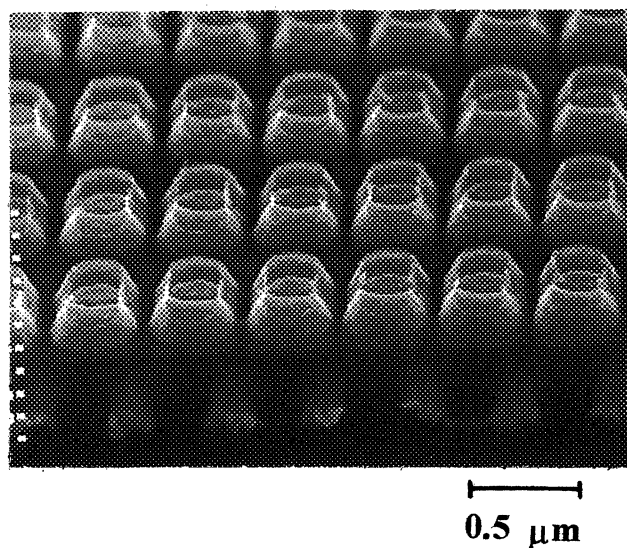


Fig. 7. Pt patterns integrated into the 0.25 μm device structure.

ing the etching of Pt at various RF powers. After a 30% overetch, Pt in the capacitor structures was completely patterned. The SEM micrograph in Fig. 7 shows the Pt electrodes of the 0.25 μm design rule after etching in Ar/Cl<sub>2</sub>/O<sub>2</sub>, removing the mask oxide, and subsequent cleaning in 20% HCl.<sup>7)</sup> The etch slope was about 65° for Pt of thickness 1000 Å. The integration process was followed by the deposition of BST as a dielectric material and Pt as a plate electrode. It was possible to etch the BST films at the etch rate of 500 Å/min in the Cl<sub>2</sub>/Ar plasma.

### 4. Discussion

The etch process led to difficulty in implementing Pt into subquarter micron devices, generating redeposits on the sidewall and resulting in etch slopes below 70°. We found that when Cl<sub>2</sub> was added to Ar, the sidewall redeposits could be removed by post-etch treatments, although the etch slope was lowered to about 45°. It is understood that the redeposits were formed heterogeneously by a combination of gases, etch products, and mask materials that eroded during the etch process,<sup>2)</sup>

resulting in rather easy removal after etching. However, this resulted in the formation of thick redeposits and consequently in less steep etch slope. With the addition of  $\text{Cl}_2$ , the mask was more laterally eroded as the etch process proceeded. This could decrease the etch slope of Pt in the extension of the mask profile. If we do not consider the mask erosion in determining the etch slope, the change of the mask shape to a tapered one may suppress the sidewall redeposition of the etch product.<sup>10)</sup>

In the  $\text{Cl}_2/\text{O}_2/\text{Ar}$  plasma, oxygen is assumed to increase the etch slope by increasing the selectivity of Pt with respect to the oxide mask via suppression of the etching of the oxide mask (Fig. 5). Since the etch slope of the substrate tends to extend from the mask slope, it is desirable to minimize mask erosion to realize near-vertical etch profiles. Consequently, process parameters that control the etch selectivity of Pt with respect to the mask, for example,  $\text{O}_2$  concentration and pressure, were found to be effective for obtaining the desirable etch profiles.

It appears that the redeposits generated during the etching of Pt can be removed by suitable plasma processes and post-etch treatments. For fluorine-rich plasmas the sidewall redeposits were found to be mainly composed of the sputtered Pt atoms (as evidenced by AES spectra of Fig. 3), which were hardly removed by either ashing or wet cleaning. For chlorine-rich plasmas containing more than 40%  $\text{Cl}_2$ , the sidewall redeposits were expected to be a mixture of Cl, mask materials, as well as the sputtered Pt. These mixture-like redeposits were removed by subsequent ashing and wet cleaning. However, it is difficult to conclude whether or not  $\text{PtCl}_x$  was formed during the etching, because the etch rate was not increased by the addition of  $\text{Cl}_2$ . It remains unclear if oxygen assisted in forming the removable sidewall redeposits,<sup>7)</sup> based on the fact that it had already been removed by the  $\text{Ar}/\text{Cl}_2$  process.

A plausible approach to avoid the redeposition of the etch product on the sidewall will be to form the sloped mask before the etching of Pt, as suggested in the redeposition model.<sup>10)</sup> According to this model, certain combinations of etch product, mask, and etchant gas with a low sticking coefficient can result in less redeposition and high etch slopes. However, this model needs to be modified for the chlorine-rich process which involves significant mask erosion, since the slope of the mask sidewall is reduced by the side erosion, and mask materials are intermixed with redeposits, forming a low density of etch products on the sidewalls. The model to determine the etch slope with mask erosion is being developed, and will be published elsewhere.<sup>11)</sup>

The etch products generated during the etching of Pt were not efficiently removed, and they were deposited

onto the chamber walls as well as onto the pattern sidewalls. Also, the etch products contaminated the subsequent process wafers, by generating particles and Pt-containing deposits on the wafer. This was confirmed from the progressive deterioration of the wafers. Also, it was interesting to detect changes in the optical emission intensity as a means of determining the endpoint because the de-excitation of  $\text{Pt}^*$  is known to be very weak. Nishikawa *et al.*<sup>4)</sup> observed the 3064 Å emission line of Pt at 0.4 mTorr. Although the emission at 3064 Å was cited to be one of the strongest Pt emissions,<sup>12)</sup> we were not able to detect it above 5 mTorr in both electron cyclotron resonance (ECR) and MERIE plasmas. Instead, the emission at 3406 Å was always detected in the plasmas investigated in this work.

## 5. Conclusions

The reactive ion etching of Pt in  $\text{Ar}/\text{CF}_4/\text{Cl}_2/\text{O}_2$  plasmas proceeded predominantly by the sputtering. The addition of  $\text{Cl}_2$  to Ar led to the formation of removable redeposits on the pattern sidewall, while the addition of  $\text{O}_2$  to  $\text{Ar}/\text{Cl}_2$  improved the etch slope of the Pt pattern up to 70°. An increase in the etch slope made it possible to integrate the Pt/BST/Pt capacitors into 0.25 μm devices.

- 1) T. Eimori, Y. Ono, H. Ito, T. Nishimura, T. Horikawa, T. Shibano, K. Sato and T. Nanba: *Nikkei Microdevices*, February (1994) **99** [in Japanese].
- 2) T. Shibano and K. Nishikawa: *Oyo Buturi* **63** (1994) 1139 [in Japanese].
- 3) R. Khamankar, B. Jiang, R. Tsu, W.-Y. Hsu, J. Nulmen, S. Summerfelt, M. Anthony and J. Lee: *Symp. VLSI Technol. Dig. Tech. Papers* (1995) p. 127.
- 4) K. Nishikawa, Y. Kusumi, T. Oomori, M. Hanazaki and K. Namba: *Jpn. J. Appl. Phys.* **32** (1993) 6102.
- 5) K. Tokashiki, K. Sato, K. Takemura, S. Yamamichi, P.-Y. Lesaicherre, H. Miyamoto, E. Ikawa and Y. Miyasaka: *Proc. 16th Dry Proc. Symp.* (The Institute of Electrical Engineers, Tokyo, 1994) p. 73.
- 6) S. Saito and K. Kuramasu: *Jpn. J. Appl. Phys.* **31** (1992) 135.
- 7) S. Yokoyama, Y. Ito, K. Ishihara, K. Hamada, S. Ohnishi, J. Kudo and K. Sakiyama: *Ext. Abstr. 1994 Int. Conf. Solid State Devices and Materials* (Business Center for Academic Societies, Japan, Tokyo, 1994) p. 721.
- 8) H. Aoki, T. Hashimoto, E. Ikawa, T. Kikkawa, T. Sakuma and Y. Miyasaka: *Ext. Abstr. The Jpn. Soc. Appl. Phys.* (1991) p. 516 [in Japanese].
- 9) *Glow Discharge Processes*, ed. B. Chapman (John Wiley & Sons, 1980) p. 232.
- 10) *VLSI Electronics Microstructure Science*, eds. N. G. Einspruch and D. M. Brown (Academic Press Inc., 1984) Vol. 8, p. 354.
- 11) W. J. Yoo, H. W. Kim, B. Y. Nam, C. O. Jung and Y. B. Koh: unpublished work.
- 12) *Handbook of Chemistry and Physics* (CRC Press, 1989-1990) 70th ed., E283.